HHS Public Access

Author manuscript

J Comp Neurol. Author manuscript; available in PMC 2018 February 16.

Published in final edited form as:

J Comp Neurol. 2017 December 01; 525(17): 3666–3682. doi:10.1002/cne.24295.

Distribution and chemical composition of estrogen receptor β neurons in the paraventricular nucleus of the female and male mouse hypothalamus

Mario G. Oyola[1], **Maranda K. Thompson**[2], **Aaron Z. Handa**[2], and **Robert J. Handa**[1]

[1]Department of Biomedical Sciences, Colorado State University, Fort Collins, Colorado

[2]Department of Basic Medical Sciences, Univ. Arizona College of Medicine, Phoenix, Arizona

Abstract

Activation of estrogen receptor beta (ERβ)-expressing neurons regulates the mammalian stress response via the hypothalamic–pituitary–adrenal (HPA) axis. These neurons densely populate the paraventricular nucleus of the hypothalamus (PVN). Recent research has revealed striking differences between rat and mouse PVN cytochemistry, but careful exploration of PVN ERβ neurons in mice has been hindered by a lack of specific ERβ antisera. Therefore, we used male and female transgenic mice expressing EGFP under the control of the mouse ERβ promoter (ERβ-EGFP) to examine the chemical architecture of PVN ERβ cells. Using immunohistochemistry, we found that 90% of ERβ-immunoreactivity (-ir) colocalized with EGFP. Cellular colocalization of EGFP with neuropeptides, transcription modulators, and neuronal tracers was examined throughout the PVN. ERβ-EGFP cells expressed oxytocin more abundantly in the rostral (71 ± 3%) than caudal (33 ± 8%) PVN. Arginine vasopressin colocalized with EGFP more often in females (18 ± 3%) than males (4 ± 1%). Moreover, estrogen receptor α-ir colocalized with ERβ-EGFP at low levels (15 ± 3%). Using a corticotropin releasing hormone-cre driver X tdTomato reporter mouse, we found a moderate colocalization with ERβ-ir (48 ± 16%) in the middle PVN. Peripheral injection of fluorogold revealed that the rostral PVN ERβ-EGFP cells are neuroendocrine neurons whereas non-neuroendocrine (presumably pre-autonomic) ERβ-EGFP neurons predominated in the posterior PVN. These data demonstrate chemoarchitectural differences in ERβ neurons of the mouse PVN that are different from that previously described for the rat, thus, elucidating potential neuronal pathways involved in the regulation of the HPA axis in mice.

Correspondence: Mario G. Oyola, Ph.D., Department of Biomedical Sciences, 1617 Campus Delivery, Colorado State University, Ft. Collins, CO 80523-1617., mario.oyola@colostate.edu.

ORCID

Mario G. Oyola http://orcid.org/0000-0001-5554-162X

AUTHOR CONTRIBUTIONS

All authors had full access to the data presented in this work and take responsibility for integrity of the data presented and the accuracy of the data analysis. Study concept and design: MGO, RJH. Acquisition of data: MGO, MKT, AZH. Analysis and interpretation: MGO, RJH. Drafting of manuscript: MGO. Critical revision of the manuscript for important intellectual content: RJH. Statistical analysis: MGO. Obtained funding: RJH.

Keywords

cytochemistry; estrogen receptor beta; paraventricular nucleus of the hypothalamus; ESR2; RRID: MMRRC_036904-UC; RRID:IMSR_JAX:007908

1 INTRODUCTION

First described in 1996 (Kuiper, Enmark, Pelto-Huikko, Nilsson, & Gustafsson, 1996), the beta form of estrogen receptor (ERβ) has been linked to an array of neurophysiological functions like learning and memory (Rissman, Heck, Leonard, Shupnik, & Gustafsson, 2002; Jacome et al., 2010), anxiety-related disorders (Lund, Rovis, Chung, & Handa, 2005; Oyola et al., 2011) and hypothalamic–pituitary–adrenal (HPA) axis response to stress (Weiser, Wu, & Handa, 2009). Determining the neurobiological participation of ERβ in these systems will not only require a precise understanding of ERβ's neuroanatomical organization in the brain, but also require deciphering the protein partners of ERβ, shedding light on molecular pathways that might impact ERβ's physiological effects.

Much of what we currently know of the distribution of ERβ in the brain and hypothalamus comes from studies in the rat using in situ hybridization (Laflamme, Nappi, Drolet, Labrie, & Rivest, 1998), immunohistochemistry (Shughrue & Merchenthaler, 2001), and PCR (Kuiper et al., 1997), and in the human hypothalamus using immunohistochemistry (Kruijver, Balesar, Espila, Unmehopa, & Swaab, 2003). Nonetheless, the expression pattern of ERβ protein in the brain has been somewhat controversial, mainly due to the current lack of specific antisera to directly label this nuclear receptor (Snyder, Smejkalova, Forlano, & Woolley, 2010). Nevertheless, most reports agree on one finding, across all species examined, there is a dense presence of ERβ expressing neurons in the paraventricular nucleus of the hypothalamus (PVN). This has led us to believe that this localization pattern should play a key role in the function of this nucleus.

Estrogen's biological actions are mediated by two nuclear receptors: ERα and ERβ. Estradiol has been shown to play a key role in the regulation of the HPA axis, acting through ERα and ERβ. For example, Lund et al. (2005) studied the activation of the HPA axis in ovariectomized rats using selective ERα and ERβ agonists. While ERα agonists caused hyperreactivity of the HPA axis, ERβ agonists decreased the corticosterone and adrenocorticotropic hormone (ACTH) response to stress (Lund et al., 2005). The distribution of these receptors differs across brain regions, with ERβ mRNA (Shughrue, Komm, & Merchenthaler, 1996; Laflamme et al., 1998) and protein (Li, Schwartz, & Rissman, 1997; Shughrue & Merchenthaler, 2001) expression predominating in the PVN, perhaps indicating a dominant role of PVN ERβ-mediated actions of estradiol on the activity of the HPA axis. These results in rats lead us to inquire whether these two receptors are localized in a similar fashion in the mouse PVN.

The neurons of the PVN play a central role in the control of the HPA axis. Integration of numerous signals is required to maintain effective control of this axis, which is crucial for homeostasis. Although the PVN is composed of a heterogeneous population of neurons, the main neuroendocrine players involved in the regulation of the HPA axis and shown to

interact with ERβ, are those that express oxytocin (OT), argi-nine vasopressin (AVP), and corticotropin-releasing hormone (CRH) (Handa & Weiser, 2014). These peptide hormones are critical for the proper activation and termination of HPA activity, the end result being the elevation and eventual inhibition of circulating corticosteroids.

Recent studies have pointed out anatomic similarities and dissimilarities in cyto- and chemo-architecture between rats and mice, particularly in the PVN, (Swanson & Sawchenko, 1980; Biag et al., 2012). In this study, we dissected the chemical and cytological distribution of ERβ neurons within the mouse PVN utilizing a transgenic mouse model. This ERβ-EGFP mouse model was previously described by Milner et al. (2010) and Zuloaga, Zuloaga, Hinds, Carbone, and Handa, (2014) and uses a bacterial artificial chromosome (BAC) transgenic mouse where ERβ expressing neurons can be identified by the expression of EGFP placed under control of the mouse ERβ-promoter in the BAC. In the present study, we utilized this model and further extended its validity using the highly effective antibody against ERβ (Z8P), first described by Shughrue and Merchenthaler (2001); unfortunately, this antibody has not been commercially available for many years.

In the present work, we sought to elucidate the chemical composition and distribution of ERβ-containing cells in male and female mice using a genetic approach combined with immunohistochemistry (IHC) against ERα, ERβ, tyrosine hydroxylase (TH), OT, and AVP. We found similarities and differences in the distribution of these peptides in neurons of the PVN relative to ERβ, when compared to previous studies in the rat. Moreover, our studies show some sex differences in ERβ distribution in the mouse PVN that have not been previously described in rats. This work will shed light on the underlying mechanism by which ERβ may regulate the HPA axis in the rodent.

2 MATERIALS AND METHODS

2.1 Animals

These studies utilized a BAC transgenic mouse line where EGFP is expressed under the control of the mouse ERβ promoter (ERβ-EGFP) in the BAC (RRID:MMRRC_036904-UCD). These mice allow for the study of ERβ expressing neurons using EGFP as a reporter (Milner et al., 2010; Zuloaga et al., 2014). ERβ-EGFP mice were developed by Dr. Nathaniel Heintz (The Rockefeller University, NY) and acquired from the Mutant Mouse Regional Resource Center at the University of California, Davis. Validation and fidelity of this mouse model was previously described (Milner et al., 2010) and expression in the hypothalamus was further confirmed and extended in this work by immunohistochemistry. For our studies, the original ERβ-EGFP mouse from MMRRC was backcrossed onto a C57bl6/J strain for at least ten generations, whereas the ERβ-EGFP mice used by Milner et al. (2010) were backcrossed onto this strain for three generations.

We also used a CRH-cre driver mouse line [B6(Cg)-Crh^{tm9cre0Zjh}/J (CRH-cre) (Jackson laboratories, stock#: 012704), RRID:IMSR_JAX:012704], where the CRH promoter drives the expression of the cre recombinase enzyme. These mice were crossed to a loxP-STOP-loxP-TdTomato reporter strain [(B6.Cg-Gt(ROSA)26Sor$^{tm14(CAG-TdTomato)Hze}$/J; Ai14) (stock#: 007908, RRID:IMSR_JAX:007908) (Jackson Laboratory, Bar Harbor, ME)],

allowing for expression of the fluorescent protein, TdTomato, in cre-expressing cells. Both of these transgenic lines are on a C57bl6/J background. The use of this cross to accurately locate hypothalamic CRH expressing neurons under physiological conditions has been previously described (Wamsteeker Cusulin, Fuzesi, Watts, & Bains, 2013; Smith et al., 2014).

2.2 Genotype

At weaning, ear punches were made for identification and the tissue was used for genotyping. ERβ-EGFP mice were genotyped following a protocol developed by MMRRC (http://mmrrc.ucdavis.edu/doc/GEN-SAT-EGFPGeno_Protocol.pdf) using the following nucleotide primer sequences: Forward ESR2: TCT GAG ACT GCA TCT CTG TAG TCC AA and Reverse GFP: TAG CGG CTG AAG CAC TGCA. CRH-Cre and mice were genotyped following the Jackson Laboratory protocol. CRH-cre PCR primers: Common: CTT ACA CAT TTC GTC CTA GCC, Reverse wild type: CAC GAC CAG GCT GCG GCT AAC, Mutant forward: CAA TGT ATC TTA TCA TGT CTG GAT CC.

The Ai14 reporter strain was genotyped using the following primer sets: AAG GGA GCT GCA GTG GAG TA (WT Forward), CCC AAA ATC TGT GGG AAG TC (WT Reverse), GGC ATT AAA GCA GCG TAT CC (Mutant Forward), and CTG TTC CTG TAC GGC ATG G (Mutant Reverse).

Mice used in these studies were bred in the laboratory animal research facilities at the University of Arizona College of Medicine -Phoenix and Colorado State University and housed under 12-hr light, 12-dark photoperiod (lights on at 6 a.m.). Experimental animals were weaned at 21 days of age and multiple housed in same sex cages in temperature and humidity controlled rooms. Animals had ad libitum access to water and food (Teklad-2918, Envigo, Indianapolis, IN). All procedures were approved by the Institutional Animal Care and Use Committee at the University of Arizona and at Colorado State University.

2.3 Tissue harvesting and processing

Male and randomly cycling female mice were anesthetized with isoflurane and intracardially perfused with 1X PBS (pH 7.5) followed by 4% buffered paraformaldehyde (PFA). Their brains were removed from the skull and post-fixed in 4% PFA overnight. Brains were subsequently switched into a 30% sucrose antifreeze solution until infiltrated. Four series of 35 μm thick sections through the PVN were acquired using a Leica CM3050S cryostat (Buffalo Groove, IL) and processed for immunohistochemistry using standard procedures.

2.4 Immunohistochemistry (IHC)

Immunohistochemistry was performed for; ERβ, OT, ERα, TH, GFP, and AVP (Table 1). Free floating tissue sections were rinsed with 1X PBS (pH 7.5) and then blocked for one hour in PBS containing 5% NGS and 0.1% Triton X-100, then incubated in primary antibody in 1X PBS-T (pH 7.5, 0.1% Triton X-100) overnight with gentle shaking, with the exception of the TH antibody, which was incubated with tissue sections for 48 hr at 4°C. Subsequently, tissue sections were rinsed three times for ten minutes in 1X PBS-T. Tissue sections were incubated with a secondary antibody, as described in Table 1, for one hour,

then again washed three times for 10 min in 1X PBS-T. One final wash was performed in 1X PBS before mounting the slices using VectaShield™ (Vector Laboratories, Burlingame, CA)

Tissue intended for ERβ immunohistochemistry was treated with 0.3% hydrogen peroxide for 30 min prior to the blocking step described above and incubation with ERβ Z8P (originally obtained from Zymed Laboratories Inc., South San Francisco, CA) and this same lot was used in previous studies examining ERβ in the rat PVN (Suzuki & Handa, 2004; Suzuki & Handa, 2005). Incubation occurred in 1X PBS-T overnight. The following morning, tissue sections were washed three times for 10 min in 1X PBS-T, then processed using the Vector ABC Elite protocol. For development, a tyramide (Tyramide Signal Amplification Fluorescein or Cy3 System; Perkin Elmer, Waltham, MA) amplification step was performed for 8 min, followed by three 10-min washes in 1X PBS-T and two final rinses in 1X PBS.

Nuclear counterstaining was achieved using TO-PRO-3 Iodide (ThermoFisher, Waltham, MA). After the final step of the IHC procedures described above, tissue sections were incubated in TO-PRO-3 in 1X PBST (1:1,000) for 30 min. Sections were then washed three times for 10 min in PBST with an additional final two washes in 1X PBS. Slices were then mounted onto glass slides and coverslipped with VectaShield™.

Some sections were not immunoreacted and were stained for Nissl substance by using 0.1% toluidine blue following standard dehydration processing and subsequently they were coverslipped using Permount (Fisher Scientific, Waltham, MA).

2.5 Antibody characterization

Detailed antibody information on manufacturer, lot and catalog number, immunogen, and RRID can be found in Table 1. Additional evidence of the antibodies' specificity is provided below.

2.5.1 ERβ Z8P—This antibody was extensively used in the rat when it was commercially available, and it proved to be one of few highly specific antibody to ERβ (Shughrue & Merchenthaler, 2001; Suzuki & Handa, 2004; Suzuki & Handa, 2005). To ensure that the ERβ Z8P antibody was also specific in mouse, we used a global ERβ knockout (βERKO) and WT mouse, and followed the aforementioned IHC procedure for ERβ Z8P. No ERβ signal was detected in coronal sections from the βERKO mouse, confirming previous studies (McClellan, Stratton, & Tobet, 2010). This antibody has also been used previously to detect ERβ in mouse brain (Goto et al., 2003).

2.5.2 OT—The OT antibody (RRID:AB_518524) was produced in rabbits immunized with the full length synthetic OT peptide. This antibody's cross-reactivity was determined by the manufacturer (Bachem/Peninsula Lab) using radioimmunoassay in different species, ranging from the mouse and rat to sheep, bovine, horse, porcine, and human. The appropriate characterization (as per Saper & Sawchenko, 2003) was performed by Griffin et al., where preabsorption controls and IHC in OT KO mouse model failed to detect the OT-ir (Griffin, Ferri-Kolwicz, Reyes, Van Bockstaele, & Flanagan-Cato, 2010). Furthermore, the OT-ir

signal detected in our work was similar to that observed in previous studies (Kadar et al., 2010; Chee, Pissios, & Maratos-Flier, 2013)

2.5.3 AVP—This antibody was generated by Norman Kasting and Joseph Martin (Kasting & Martin, 1983; Kasting, Mazurek, & Martin, 1985) and provided to us by Dr. James I Koenig (Univ. Maryland). Specificity was checked by preadsorption of the antibody with mouse AVP (1 μg/mL; Phoenix Pharmaceuticals, Burlingame, CA) prior to IHC, or omission of the primary antibody, both of which prevented any immunoreactive signal. Moreover, the pattern of AVP-ir distribution in the hypothalamus was similar to that observed in previous studies (Vacher, Fretier, Creminon, Calas, & Hardin-Pouzet, 2002; Biag et al., 2012).

2.5.4 ERα—The antiserum for ERα used in this work recognizes a 64–66 kDa band in immunoblot of processed cells transfected COS-1 cells, and not in control untransfected cells (Friend, Resnick, Ang, & Shupnik, 1997). Papka et al. (2002) showed that preabsorption with ERα, and not ERβ, protein avoided ir in IHC studies using rat brains (Papka & Storey-Workley, 2002). In addition, the ERα-ir distribution shown in our study is similar to that shown by others using the mouse (McClellan et al., 2010).

2.5.5 GFP—This antibody was generated against recombinant GFP. The manufacturer (Aves Lab Inc., Tigard, OR) specified that this anti-chicken antibody is specific against the recombinant GFP using immunoblot. Also, Encinas, Vaahtokari, and Enikolopov (2006), have shown that it recognizes the gene product of GFP-expressing transgenic mice similar to the one used in the current study (Encinas et al., 2006). Volkmann et al., have also demonstrated an absence of GFP labeling in zebra fish not carrying the GFP construct (Volkmann, Chen, Harris, Wullimann, & Koster, 2010), confirming specificity for GFP.

2.5.6 TH—A synthetic peptide corresponding to the rat TH, amino acids 32–47, was used to generate the antibody. The expression pattern and number of TH-positive cells detected matched those observed in Kiss, Mravec, Palkovits, and Kvetnansky (2008), particularly in the PVN (Kiss et al., 2008).

2.6 Microscopy, 3D analysis, and mapping

All images (excluding the tracing experiment using fluorogold [FG] and Nissl staining) were acquired with a Zeiss 880 Laser Scanning Microscope (LSM) using a Plan-Apochromat 10× objective and 1.4× digital magnifications. Images acquired to visualize FG/ERβ-EGFP were obtained with a Zeiss LSM 880 inverted using a Plan-Apochromat 20× objective and 0.8× digital magnification. Nissl stained photomicrographs were acquired with Zeiss Imager Z2 using a Plan-Apochromat 5X objective, a Axiocam 506 mono camera, and Zen 2.3 Pro software.

Images of the PVN were acquired with the z-stack module using Zeiss Zen 2.1 software. The z-thickness sampling interval was matched to the pixel size of the images (512 × 512) to allow square voxels for optimal imaging. To keep uniformity and avoid sampling the most superficial layers of the brain slices, the total scanned z-stack distance was 20 μm per brain section. Each channel used was scanned individually to prevent crosstalk between channels and fluorophores.

Rostral, middle, and caudal portions of the PVN were partitioned using anatomical landmarks visible after TO-PRO-3 nucleic acid staining (Figure 1). This staining, as with other non-fluorescent staining, aids in the visualization of fluorescent immunoreactive distribution in the PVN by marking the boundaries of the nucleus. The rostral, middle, and caudal levels of the PVN were outlined after TO-PRO-3 staining, and subsequently the level was assigned a portion approximately equivalent to 1/3 of the rostral–caudal distance through the PVN to each of these regions. One section per zone per subject was analyzed.

All images were analyzed using the 3D imaging software, Imaris 8.1.2 (Bitplane AG, RRID:SCR_007370) by applying a mask that fit the reproducible anatomical shape of the region being analyzed using the TO-PRO-3 staining. This mask allows us to study ERβ cells in the PVN and avoid the quantification/study of cells outside the PVN. Images were optimized for each neuropeptide analyzed to allow for optimal signal determination. The colocalization analysis was performed using the Coloc module from Imaris 8.1.2, where labelled cells were auto located, and these cells further verified by an individual investigator, blinded to treatment group to correct any mislabeled or unlabeled cells. Labeled cells were marked by a spot placed in the center of the cell for each of the neuropeptide signals. The colocalization module was used to determine colocalization using the center of the spot. Spot centers equal to, or less than 5 μm apart were deemed colocalized by the software and then verified manually, using the 3D view in Imaris.

2.7 Neuroendocrine versus non-neuroendocrine

To determine whether ERβ PVN neurons are neuroendocrine, ERβ-EGFP animals were subcutaneously injected with 50 μL of 5% FG (Fluorochrome, Denver, CO) in saline (0.9%) according to previously published approaches (Kriegsfeld, Korets, & Silver, 2003). Five days later, animals were perfused intracardially using 4% PFA, and their brains were removed, postfixed and cryoprotected and then cryosectioned and processed for immunohistochemistry using the anti-GFP antibody. Since neurosecretory PVN cells projecting to the medial eminence have terminals that are outside the blood brain barrier, they can pick up the circulating tracer and retrogradely transfer FG back to the cell soma, as previously described (Kriegsfeld et al., 2003).

2.8 Statistics

All data are presented as mean +/− the standard error of the mean (SEM). Counts of immunoreactive and reporter gene-labeled cells were analyzed using a two-way analysis of variance (ANOVA) (PVN region X sex) using GraphPad Prism version 6.0h for Mac (GraphPad Software, San Diego, CA). Post hoc analysis was accomplished using the Bonferroni correction method. $p < .05$ was considered significant.

3 RESULTS

3.1 ERβ-EGFP mouse model is a valid tool for studying PVN ERβ expression

In this study, we further validated the ERβ-EGFP mouse model (Milner et al., 2010; Zuloaga et al., 2014) in the PVN qualitatively and quantitatively, using a previously described antibody that effectively recognizes the C-terminus of the ERβ protein (Z8P; Shughrue &

Merchenthaler, 2001; Suzuki & Handa, 2005). ERβ-EGFP positive cells showed more than 90% colocalization with ERβ-ir cells throughout the PVN (Figure 2). This near perfect overlap indicates the high specificity of EGFP expression that corresponds with presence of ERβ protein. Figure 2 also shows the cellular location of EGFP in the cytoplasm in comparison to the nuclear staining of the immunolabeled ERβ protein. The Z8P antibody was further validated for mouse brain by using IHC to show the presence of ERβ-ir in the PVN of a WT mouse, but an absence of labelling in the βERKO mouse (Figure 3).

Neuronal cell counts revealed that there was no apparent sex difference in the relative number of ERβ-EGFP neurons in the PVN, consistent with previous studies (Milner et al., 2010). However, the distribution of ERβ-EGFP differed significantly between the rostral–caudal extent of the PVN (2-way ANOVA [region × sex]; Region: ($F_{(2,203)}$ = 29.02); p <. 0001), with the highest amount of ERβ-EGFP cells in the caudal PVN. There was no effect of sex ($F_{(1,203)}$ = 0.088; ns) or interaction ($F_{(2,203)}$ = 0.886; ns). We detected an average of 84.0 ± 6.5 ERβ-EGFP neurons per section in the rostral part of the PVN, 84.5 ± 6 in the middle PVN and 127 ± 7 in the caudal PVN of ERβ-EGFP mice.

3.2 OT colocalizes with PVN ERβ-EGFP cells in an PVN region-specific manner

Using immunocytochemistry to detect OT expressing neurons, we discovered that the number of ERβ-EGFP neurons that coexpressed OT differed with the anatomic level of the PVN. Two-way ANOVA of colocalized cell numbers revealed a significant effect of the region of the PVN ($F_{(2,9)}$ = 29.30 (p < .0001), but no sex ($F_{(1,9)}$ = 1.879; ns) or interaction effect ($F_{(2,9)}$ = 2.674; ns). The rostral part of the PVN (rPVN) showing highest colocalization between ERβ and OT (70 ± 5% average in female and 73 ± 1.7% in males), whereas the least colocalization was seen in the caudal PVN (cPVN) (34 ± 4.5% average in females and 32 ± 7.5% in males) (Figure 4). The middle PVN (mPVN) showed an average colocalization of 52 ± 5% in females and 32 ± 0.5% in males. Conversely, the majority of OT cells expressed ERβ independent of PVN region ($F_{(2,9)}$ = 0.004; ns) or sex ($F_{(1,9)}$ = 0.029; ns). Male and female mice had similar levels of colocalized ERβ in OT cells, averaging from 81 ± 2.5% in the rPVN and 76 ± 6.4%, to 81 ± 7.15% in the cPVN.

3.3 AVP colocalizes with PVN ERβ-EGFP cells in a sex and region specific manner

Cell counts following IHC for AVP revealed that the density of ERβ-EGFP cells that also expressed AVP within the PVN was rather sparse compared to oxytocin (Figure 5). 2-way ANOVA revealed a significant effect of sex across PVN regions ($F_{(1,15)}$ = 13.96; p = .002). Furthermore, a significant effect of region on colocalized AVP/ERβ-EGFP cells was seen ($F_{(2,15)}$ = 11.01; p = .001) but no interaction effect was observed ($F_{(2,15)}$ = 3.583; p = .053). The greatest number of AVP/ERβ-EGFP neurons were present in the rPVN (14 ± 3.1% females and 8 ± 3.3% in males), followed by the mPVN (18 ± 3.2% in females and 3.6 ± 1.4% in males), and then the cPVN (2 ± 1.1% in females and 0.2 ± 0.2% in males). Interestingly, a similar pattern (females > males) was observed in the percent of AVP cells that expressed EGFP ($F_{(1,15)}$ = 7.682; p = .0143). However, the highest number of ERβ-EGFP/AVP cells was found in the cPVN (45% in females and 11% in males), in contrast to the rPVN where the greatest number of AVP/ERβ-EGFP colocalized cells were found.

3.4 ERα/ERβ-EGFP colocalized cells are present in low levels in the male and female mouse PVN

ERα-ir cells were detected through all regions of the PVN with no readily identifiable distribution pattern (Figure 6). A two-way ANOVA showed no effect of sex ($F_{(1,15)}$ = 1.162; ns), PVN region ($F_{(2,15)}$ = 0.811; ns) or interaction ($F_{(2,15)}$ = 0.43; ns) in the percent of colocalized ERα/ERβ-EGFP. The ERα/ERβ-EGFP colocalization percentage was as followed: rPVN= 23 ± 13.6% in females and 8 ± 3.2% in males, mPVN= 16 ± 2.6% in females and 15 ± 3.1% in males, and cPVN= 27 ± 4.8% in females and 22 ± 9.3 in males. However, there were significantly higher percentages of ERα cells that expressed ERβ-EGFP in the cPVN of both male (52%) and female (38%) mice (main effect of PVN region: $F_{(2,9)}$= 28.33; p < .001) compared to the rPVN or mPVN.

3.5 Tyrosine Hydroxylase is not present in PVN ERβ-EGFP cells

Although TH-ir cells were concentrated in the rPVN and mPVN, ERβ-EGFP cells in the PVN of male and female mice did not express TH in any of the PVN regions studied in this work (Figure 7).

3.6 CRH/ERβ-ir colocalized neurons are moderately present in the male and female mouse PVN

To determine the expression of CRH by ERβ PVN cells we used a CRH-*IRES*-cre mouse crossed to a TdTomato reporter mouse (Ai14), which results in the labeling of CRH-expressing cells with TdTomato (Figure 8). In this study, it was important to use the Z8P antibody to detect ERβ-ir. Two-way ANOVA revealed that the percentage of tdTo-mato/ERβ-ir cells significantly differed depending on the PVN region ($F_{(2,6)}$ = 7.504; p = .0233). No effect of sex ($F_{(1,6)}$ = 0.018) or interaction ($F_{(2,6)}$ = 0.056) was observed. The highest percentage of CRH-cre/ERβ-ir cells was observed in the mPVN (45 ± 12.1% in females and 51 ± 20.9% in males), followed by the cPVN (33 ± 16.3% in females and 33 ± 3.9% in males), and lastly the rPVN (3 ± 3.3% in females and 1 ± 0.5% in males). A similar distribution pattern was observed in the number of ERβ-ir/tdTomato cells, but we found a significant effect of PVN region ($F_{(2,6)}$ = 8.962; p = .015) where almost no tdTomato-positive cells in the rPVN contained ERβ (0.4 ± 0.4% in females and 0.2 ± 0.1% in males), the mPVN contained 38 ± 1.9 in female and 32 ± 7% in males, and similar numbers were found for the cPVN (28 ± 20.1% in females and 36 ± 6.1% in males). Of note, the total number of ERβ cells is very low relative to the number of CRH cells in the rPVN.

3.7 Neuroendocrine ERβ neurons are highly present in the rostral portion of the PVN

The retrograde tracer, FG has been shown to be taken up by neuroendocrine neurons that project outside the brain blood barrier at the median eminence (Kriegsfeld et al., 2003), making it an excellent way to identify neuroendocrine cell of the PVN following peripheral administration of the retrograde tracer FG (Figure 9). Two-way ANOVA showed that ERβ-EGFP cells that were labeled following peripheral FG injection showed a significant and distinct distribution in the PVN (Region: $F_{(2,14)}$= 17.01; p = .0002), with the highest concentration of FG/ERβ-EGFP colocalized cells in the rPVN (54 ± 1.6% in females and 72 ± 2.8% in males), followed by the mPVN (48 ± 24.8% in females and 24 ± 3.0% in males),

and lowest levels in the cPVN (6 ± 1.8% in female and 9 ± 0.5% in males). No effect of sex ($F_{(1,14)}$ = 0.014; ns) or interaction ($F_{(2,14)}$ = 2.574, ns) was observed.

4 DISCUSSION

In the current study, we used and validated a transgenic mouse model, ERβ-EGFP, that allowed for the accurate identification of ERβ neuronal distribution and chemical composition in the PVN of male and female mice. The use of this mouse model has been previously described by several others (Milner et al., 2010; Zuloaga et al., 2014; Marques-Lopes et al., 2015). The distribution of EGFP in this mouse model faithfully recapitulates the distribution of ERβ-ir and mRNA in many areas of the rat and mouse brain, which corresponds with our findings that ERβ-ir and ERβ-EGFP expression are near identical in the PVN. We showed that ERβ cells in the mouse PVN expresses OT, CRH, AVP, and ERα in a PVN-region-specific manner. Interestingly, we noted significantly higher level of colocalized AVP and ERβ cells in female mice, compared to males, perhaps indicating a potential role of AVP in the estradiol-dependent sex differences present in the HPA axis reactivity. Lastly, we showed that the majority of ERβ cells in the rostral PVN are neuroendocrine cells, suggesting a potential role of ERβ in these cells, whose secretory product ultimately impacts cells in the anterior pituitary, to control the HPA axis and other neuroendocrine secretory loops.

Previous studies describing the chemical and cytological distribution of ERβ in the brain have been largely restricted to rat studies and differing results from these studies are common, for a number of reasons including: (a) the usage of different ERβ antisera with unlike specificities (Snyder et al., 2010), (b) the lack of comparison with opposite sex conspecifics, (c) the sensitivity of the technique utilized, and (d) the use and comparison of different species. Thus, identifying a valid model for the study of ERβ, determining the main discrepancies across species, and surveying differences between male and female subjects will advance our understanding of the function of ERβ in the brain.

The PVN of the rodent houses two main neuronal populations, neuroendocrine and pre-autonomic neurons, each with a wide variety of phenotypes. Neurosecretory neurons in the PVN, like CRH (Fuzesi, Daviu, Wamsteeker Cusulin, Bonin, & Bains, 2016), OT (Dabrowska et al., 2011) and AVP (Goncharova, 2013) are known to be directly linked to the up- or down-regulation of the HPA axis through projections to the hypothalmo-hypophyseal portal vasculature. In the rat, PVN neuronal populations are distributed in a spatially specific manner, however, in other species, like mice and humans, this distribution is not as well-defined. Of importance for this study, the PVN houses an abundant number of neurons that express ERβ, leading us to hypothesize that ERβ may play a key role in the regulation of the HPA axis at this level (Handa, Mani, & Uht, 2012).

Estradiol's peripheral and central actions are directed by the two main types of ER: ERα and ERβ. In females, ovariectomy, which depletes gonadal hormone levels, results in a reduced ACTH and CORT response to restraint stress (Burgess & Handa, 1992; Goncharova, 2013). These effects are reversed by estradiol treatment, which increases the HPA axis response to stress (Burgess & Handa, 1992; Handa, Burgess, Kerr, & O'Keefe, 1994). However, other

studies have shown the opposite. For example, estradiol treatment can attenuate the HPA axis response to stress (Figueiredo, Dolgas, & Herman, 2002; Ochedalski, Subburaju, Wynn, & Aguilera, 2007). These dichotomous estradiol actions may result from its independent or combinatorial actions on ERα and/or ERβ. Using pharmacological and genetic approaches to further dissect the function of each of these receptors on the HPA axis, we have previously shown that treatment with the selective ERβ agonist, DPN, can decrease anxiety-like behaviors and hyperactivation of the HPA axis in ovariectomized rats (Lund et al., 2005) and mice (Oyola et al., 2011). In addition, ERα agonists (Lund, Hinds, & Handa, 2006) can modulate these responses and increase the response to stressors, presumably through interactions in and around the PVN (Weiser & Handa, 2009). Thus, interrogating the specific distribution of ERβ neurons in the mouse and identifying its neuropeptide mediators is imperative for the understanding of how ERβ might be modulating both of these physiological responses.

In these studies, we used a polyclonal antibody against ERβ (Z8P), which was used previously to describe the distribution of ERβ in several neurobiological systems in the rat. This antibody has not been available for over a decade and unfortunately, as pointed out by Snyder et al. (2010), newly developed antibodies have been unsuccessful with IHC in complex tissues like the brain. They showed that most of the available ERβ antisera equally detect ERβ by western blot analysis in wild type, as well as in the complete ERβ knockout mice (βERKO) and $ERβ_{ST}^{L-/L-}$null mouse. To circumvent the difficulty in detecting ERβ-ir in brain, we have used an ERβ-EGFP mouse model for our studies. Initially, to determine whether, in our hands, this mouse line accurately models the distribution of ERβ in PVN we used stocks of the Z8P antibody that we initially used to describe ERβ-ir distribution in the brain of the rat (Solum & Handa, 2002; Suzuki & Handa, 2004). We showed that this antibody can detect ERβ in wild type but not BERKO mice, as previously reported (McClellan et al., 2010), and we also found that the percentage of immunolabeled-ERβ and ERβ-EGFP neurons was greater than 90%. This is consistent with the original study describing the ERβ-EGFP mouse (Milner et al., 2010) who showed a similar small number of non-immunoreactive ERβ–EGFP cells. We also verified the observations of Milner et al. (2010) that, the distribution of ERβ-EGFP cells in mice recapitulated that of ERβ mRNA and protein described in the rat PVN (Shughrue et al., 1996; Alves, Lopez, McEwen, & Weiland, 1998; Laflamme et al., 1998; Shughrue & Merchenthaler, 2001). We observed that ERβ-EGFP cells in the PVN are distributed in a region-specific manner, with the highest amounts present in the cPVN and the lowest in the rPVN. Furthermore, and in accordance with the findings of Milner et al. (2010) the numbers of ERβ-EGFP neurons was similar in male and female mice (Milner et al., 2010). These results and those of others indicate that the distribution or ERβ is well conserved in the rat and mouse PVN and across sexes.

4.1 Colocalization of OT with PVN ERβ-EGFP cells in the mouse PVN

The PVN houses a large concentration of neurons containing OT—a nonapeptide that has been shown to reduce anxiety as well as inhibit the activation of the HPA axis in response to stress (McCarthy, McDonald, Brooks, & Goldman, 1996; Neumann, Krömer, Toschi, & Ebner, 2000a; Windle et al., 2004). These anxiolytic actions of OT are enhanced by estradiol in the mouse (McCarthy et al., 1996) and the rat (Kudwa, McGivern, & Handa, 2014).

Previous studies have established a strong relationship between OT and ERβ, with early studies establishing that the OT promoter is under estrogen regulation (Richard & Zingg, 1990; Burbach et al., 1994). In addition to estrogen, the androgen metabolite and ERβ selective ligand, 5α androstan-3β, 17β-diol (3β-diol), has been shown to increase OT mRNA levels in the rat PVN and drive the OT promoter in vitro (Hiroi et al., 2013). Since intracerebral OT administration into the PVN inhibits the HPA axis in male and female rats, (Neumann, Wigger, Torner, Holsboer, & Landgraf, 2000b), the high levels of OT neurons that express ERβ would suggest that OT is a potential mechanism by which ERβ neurons can inhibit the HPA axis.

In the current report, we show the highest levels of OT/ERβ colocalized neurons in the rPVN, followed by the mPVN—regions that also contain the highest numbers of ERβ neuroendocrine (FG-positive) neurons. Similarly, Biag et al. demonstrated that almost all the OT neurons located in the equivalent region of the male mouse PVN were neuroendocrine neurons (Biag et al., 2012). Interestingly, we detected a high percentage of ERβ-EGFP cell that are also OT positive in male and female mice, consistent with the hypothesis that ERβ could be modulating the activation of OT cells in the PVN. Laflamme et al. showed that in the intact male and female rats, a large percentage OT cells also express ERβ (Laflamme et al., 1998) in the ventro- and dorsomedial PVN. We found the highest OT/ERβ colocalization in the rPVN, a region composed of the medial and anterior parvicellular parts of the PVN, as described in the rat. This group noted that the percentage of OT cells that are also ERβ-positive was about 40% in the ventromedial parvocellular PVN, 15–20% in the caudal parvocellular PVN, and nonexistent in the rostral PVN. In contrast, IHC studies in the intact female rat showed more than 80% ERβ/OT colocalization in the medial parvi-cellular PVN (Suzuki & Handa, 2005).

In the current study, the percentage of OT cells that also contain ERβ-EGFP is more than 80% through the PVN of both male and female mice. It is possible that the observed differences in ERβ/OT colocalization might be due to use of intact versus gonadectomized animals. Moreover, from the high percentages of colocalized ERβ/OT and OT/ERβ, it is not surprising that several reports have demonstrated a strong interaction between ERβ and OT in mice. For example, gonadectomized male (Nomura, 2002) and ovariectomized female mice (Patisaul, Scordalakes, Young, & Rissman, 2003) treated with estradiol show elevated levels of OT mRNA in the PVN. Further, the effect of estradiol is not found in βERKO mice, suggesting ERβ involvement. Our laboratory has demonstrated that ERβ and OT work together to reduce anxiety-like behaviors and HPA axis responses to restraint stress in female rats (Kudwa et al., 2014). Moreover, this interaction may be through direct ERβ activation of the OT promoter (Hiroi et al., 2013). The strong correspondence observed between ERβ and OT suggests that these two systems could interact with each other in the PVN to set the gain of the HPA axis. However, the lack of sex differences in OT/ERβ coexpression suggests that sex differences in HPA axis reactivity may not be centered at this level.

4.2 AVP colocalizes with PVN ERβ-EGFP cells in a sex and region specific manner

Following a stressful episode, both AVP and CRH are thought to be co-released from neurons in the PVN into the hypophyseal portal vasculature to stimulate ACTH secretion from the anterior pituitary (Whitnall, 1989). AVP and CRH are key players in controlling the HPA axis (Herman, 2003). While the mechanism by which AVP regulates the HPA axis remains unclear (Goncharova, 2013), AVP has been shown to colocalize with a great number of CRH neurons in the rat PVN after depletion of circulating glucocorticoids by adrenalectomy (Kiss, Mezey, & Skirboll, 1984; Sawchenko, Swanson, & Vale, 1984). PVN CRH neurons can co-secrete AVP to activate vasopressin V1b receptor in corticotrophs, thereby augmenting the secretogogue activity of CRH on ACTH (Tanoue et al., 2004). Of note, both ERβ and ERα have been shown to differentially regulate transcription of AVP (Shapiro, Xu, & Dorsa, 2000). AVP and ERβ neurons appear to interact in the control of water balance. For instance, the level of ERβ-ir decreases dramatically in PVN and SON AVP cells after cellular dehydration caused by 2% saline consumption in rats (Somponpun & Sladek, 2004). However, there is a discrepancy in the number of colocalized AVP/ERβ versus the ERβ/AVP cells in the rat, mouse, and human. An early study reported a small percentage of ERβ neurons also expressing AVP (<5%) throughout the rat brain (Laflamme et al., 1998). This report was followed by a study using dual-IHC instead of ISH, reporting that a larger number of PVN AVP cells also contain ERβ-ir (66.14%) in the intact female rat (Suzuki & Handa, 2005). In ovariectomized rats, however, a different study reported that 88–99% of AVP cells are ERβ-ir positive (Hrabovszky et al., 2004). In contrast, in the mouse, we observed many fewer ERβ/AVP co-expressing neurons and an intriguing sex difference in the distribution of AVP/ERβ-EGFP colocalized cells in the PVN of mice. In accordance with the previous study by Milner et al. (2010) the number of AVP/ERβ-EGFP colocalized cells was relatively small, yet, we found that there were significantly higher numbers of colocalized cells in female than male PVN, even though the number of ERβ-EGFP neurons in the PVN is the same between the sexes (Milner et al., 2010). As with other neuropeptides, the distribution of these cells was significantly greater in the rPVN and mPVN (15%; 18%), where the bulk of neuroendocrine neurons lie (Biag et al., 2012). The number of colocalized ERβ-EGFP/AVP cells was also higher in female mice when compared to male conspecifics. However, the highest amount of ERβ-EGFP/AVP colocalized cells in female mice was found in the cPVN (45%), which is where pre-autonomic neurons reside (Biag et al., 2012) in the mouse PVN. These findings suggest that some of the sex differences observed in the HPA axis activation in female mice might result from the distinctive amount of AVP present in ERβ cells in their PVN. Since ERβ has been shown to inhibit AVP secretion in hypothalamic-neurohypophyseal system explants (Sladek & Somponpun, 2008), it is possible that AVP might be mediating HPA axis activity through an ERβ-dependent pathway. Intriguingly, even though we found very low levels of AVP/ERβ colocalized neurons in the mouse PVN, Nomura and colleagues reported that estradiol benzoate treatment significantly increased the levels of AVP transcript in the PVN of wild-type male mice (Nomura, 2002), through an ERβ mechanism. Consistent with this, ERβ has been shown to regulate the AVP promoter in both a ligand-dependent and ligand-independent fashion (Pak, Chung, Hinds, & Handa, 2007). These findings demonstrate a significant interaction between ERβ and AVP, which, even with low colocalized levels, regulate HPA axis activity, perhaps in a sex-dependent manner.

4.3 Distribution of ERα/ERβ-EGFP colocalized cells in the male and female mouse PVN

To investigate the potential functional significance of an opposing interaction between the two ERs in the PVN, we determined if ERα was present in the PVN and whether both nuclear receptors coexist within the same PVN cells. Although we found a low percentage of cells that expressed both receptors in the PVN, the presence of both receptors within some cells prompts the question of whether ERα activation might influence the PVN ERβ modulated activation of the HPA axis. Previous studies have reported almost negligible levels of ERα in the PVN of intact females rats and, perhaps more importantly, that there is no overlap whatsoever between ERα and ERβ (Suzuki & Handa, 2005). In the rat, ERα is found in the peri-PVN, where it is coexpressed with GAD67, the rate-limiting enzyme for GABA synthesis (Weiser & Handa, 2009). These cells are thought to innervate parvocellular cells of the PVN (Di, Malcher-Lopes, Marcheselli, Bazan, & Tasker, 2005). We also observed ERα-ir cells in the peri-PVN in the current study, particularly in the regions surrounding the rPVN. Moreover, we also detected a moderate number of ERβ-EGFP cells that also expressed ERα within the PVN. In fact, the number of colocalized ERα/ERβ-EGFP cells reached close to 30% in the cPVN, suggesting that these two receptors might be working at two different levels—together, through direct interactions in this brain region, and at the peri-PVN level through inhibitory inputs into the PVN (Weiser & Handa, 2009). Interestingly, our observation of very low level of neuroendocrine neurons in the cPVN, suggests the possibility that the ERα/ERβ-EGFP cells detected at this level are non-neuroendocrine and hence presumably involved in modifying autonomic functions. This is consistent with the study of Stern and Zhang (2003) who showed that more than 50% of rat PVN pre-autonomic neurons express ERβ-ir (Stern & Zhang, 2003). Notably, earlier studies reported that a high number of ERβ-EGFP cells project to the preautonomic regions, particularly the spinal cord (Milner et al., 2010; Marques-Lopes et al., 2014). In recent studies, preautonomic ERβ-EGFP has been shown to be involved in modulating cardiovascular functions, presumably through the regulation of NMDA receptor trafficking (Marques-Lopes et al., 2014, 2017).

As mentioned, ERα and ERβ have opposing effects on the activation of the HPA axis (Lund et al., 2005). The ERα agonist, propyl pyrazole triol (PPT), has been shown to induce c-Fos expression in PVN CRH-expressing neurons in ovariectomized mice and rats (Thammacharoen, Geary, Lutz, Ogawa, & Asarian, 2009), and increase HPA axis reactivity to restraint in ovariectomized female rats (Lund et al., 2005). On the other hand, the ERβ agonist, diarylpropionitrile (DPN), has been shown to have the opposite effect (Somponpun & Sladek, 2003; Lund et al., 2005; Oyola et al., 2011). These opposing effects, even with the moderate presence of colocalized ERα/ERβ and ERβ/ERα cells, lead us to believe that there might be circumstances where one receptor subtype is recruited more than another, perhaps due to differences in the type and availability of ligand, thereby shifting physiological responses in a context-dependent manner.

4.4 Colocalization of CRH/ERβ-ir neurons in the mouse PVN

CRH-expressing neuroendocrine neurons in the PVN are critical for initiating the HPA axis response to stress (Denver, 2009; Fuzesi et al., 2016). These cells are involved in the classical HPA response to stress, involving the secretion of CRH to the hypophyseal portal

vasculature, which in turn activate CRFR I expressed on anterior pituitary corticotrophs to stimulate the secretion of ACTH (Muller et al., 2001). However, in a recent study, these CRH neurons have been shown to also mediate a wide variety of stress-related behaviors, which are observed on a much faster time scale than the one recruited in the classic HPA axis response (Fuzesi et al., 2016). Thus, due to the striking involvement of PVN CRH neurons in the regulation of the HPA axis, we determined the co-expression of ERβ and CRH in the same neurons of the PVN. In the rat caudolateral PVN, 60% to 90% of CRH-containing neurons have been reported to contain ERβ (Laflamme et al., 1998), while the medial parvocellular PVN contains a much lower number (13%) (Suzuki & Handa, 2004). To determine whether similar percentages of CRH/ERβ are observed in the mouse, we used a CRH-IRES-cre driver mouse line, which reliably recapitulates CRH mRNA and protein signals (Smith et al., 2014; Chen, Molet, Gunn, Ressler, & Baram, 2015). This mouse model was used to overcome the rapid CRH transport to terminals and down-regulation by endogenous glucocorticoids, which limit visualization of CRH-ir soma under most physiological conditions. In the current study, we observed a high to moderate number of colocalized CRH-cre/ERβ-expressing neurons. Of note, the highest amount of CRH-cre/ERβ-expressing neurons was found in the mPVN and cPVN of male and female mice—regions that contain relatively low levels of neurosecretory ERβ neurons. Contrasted with this, a modest number of CRH-cre containing cells were found to express ERβ. These levels are somewhat less than those described for the rat PVN (Laflamme et al., 1998). Despite the relatively low number of colocalized cells, a tight relationship still exists between CRH and ERβ in the mouse PVN. In fact, Nomura et al. reported that ERβ is involved in the upregulation of CRH mRNA transcripts in the PVN in gonadectomized male mice (Nomura, 2002). This relationship is also present in in vitro models, where ERβ has been shown to be recruited to the CRH promoter following estradiol treatment (Chen, Zhu, Meng, & Zhou, 2008) and to drive CRH promoter activity (Miller, Suzuki, Miller, Handa, & Uht, 2004). Thus, the mechanism whereby ERβ agonist treatment downregulates HPA axis in response to stress in the face of elevated CRH mRNA levels remains to be determined. However, since CRH is also expressed by pre-autonomic neurons in the PVN, the possibility exists that upregulation by ERβ may predominate in a population of CRH neurons not involved in HPA axis control.

While the current study surveyed the major PVN neuropeptide systems involved in the regulation of the HPA axis, it is important to note that other neuropeptides must still be explored. To further these studies, we have begun to survey some other neurotransmitter systems like TH, secretagogin, and membrane progesterone receptor (data not shown). However, we have, thus far, found that the number or ERβ neurons that also contain any of these neurobiological markers to be very low to negligible.

5 CONCLUSION

Although it is important to stress that “mice are not small rats,” especially when referring to the organization of the brain, some of the chemical characteristics of ERβ appear to be conserved between these two species. OT/ERβ colocalized cells, for example, are present in high levels in both species. Nonetheless, we observed differences in colocalization percentages as well as the distribution pattern for many neuropeptides. Given the increasing

number of studies indicating striking dissimilarities between the mouse and the rat, particularly in the brain (Biag et al., 2012), the results of these studies advance our understanding of the neuroarchitecture and function of ERβ cells present in the male and female mouse PVN.

Acknowledgments

This work was funded by National Institutes of Health NS039951 and DK105826. The authors would like to thank Dr. Robert Cohen (Colorado State University, Fort Collins, Colorado) for use of his LSM 880 to acquire the images used in the fluorogold detection experiment and Samuel Lane and Alexa Hughes for their expert technical assistance. We would also like to thank Dr. Stuart A. Tobet, Dr. Brent Myers, Luke Schwerdtfeger, and Sebastian Pace (Colorado State University, Fort Collins, Colorado) for their help and expertise with the Nissl experiment.

References

Alves SE, Lopez V, McEwen BS, Weiland NG. Differential colocalization of estrogen receptor beta (ERbeta) with oxytocin and vasopressin in the paraventricular and supraoptic nuclei of the female rat brain: an immunocytochemical study. Proceedings of the National Academy of Sciences of the United States of America. 1998; 95(6):3281–3286. [PubMed: 9501254]

Biag J, Huang Y, Gou L, Hintiryan H, Askarinam A, Hahn JD, … Dong HW. Cyto- and chemoarchitecture of the hypothalamic paraventricular nucleus in the C57BL/6J male mouse: a study of immunostaining and multiple fluorescent tract tracing. The Journal of Comparative Neurology. 2012; 520(1):6–33. [PubMed: 21674499]

Burbach JP, Lopes da Silva S, Cox JJ, Adan RA, Cooney AJ, Tsai MJ, Tsai SY. Repression of estrogen-dependent stimulation of the oxytocin gene by chicken ovalbumin upstream promoter transcription factor I. The Journal of Biological Chemistry. 1994; 269(21):15046–15053. [PubMed: 8195142]

Burgess L, Handa R. Chronic estrogen-induced alterations in adrenocorticotropin and corticosterone secretion, and glucocorticoid receptor-mediated functions in female rats. Endocrinology. 1992; 131:1261–1269. [PubMed: 1324155]

Cao X, Xu P, Oyola MG, Xia Y, Yan X, Saito K, … Xu Y. Estrogens stimulate serotonin neurons to inhibit binge-like eating in mice. Journal of Clinical Investigation. 2014; 124(10):4351–4362. [PubMed: 25157819]

Chee MJ, Pissios P, Maratos-Flier E. Neurochemical characterization of neurons expressing melanin-concentrating hormone receptor 1 in the mouse hypothalamus. The Journal of Comparative Neurology. 2013; 521(10):2208–2234. [PubMed: 23605441]

Chen XN, Zhu H, Meng QY, Zhou JN. Estrogen receptor-alpha and -beta regulate the human corticotropin-releasing hormone gene through similar pathways. Brain Research. 2008; 1223:1–10. [PubMed: 18597742]

Chen Y, Molet J, Gunn BG, Ressler K, Baram TZ. Diversity of reporter expression patterns in transgenic mouse lines targeting corticotropin-releasing hormone-expressing neurons. Endocrinology. 2015; 156(12):4769–4780. [PubMed: 26402844]

Dabrowska J, Hazra R, Ahern TH, Guo JD, McDonald AJ, Mascagni F, … Rainnie DG. Neuroanatomical evidence for reciprocal regulation of the corticotrophin-releasing factor and oxytocin systems in the hypothalamus and the bed nucleus of the stria terminalis of the rat: Implications for balancing stress and affect. Psychoneuroendocrinology. 2011; 36(9):1312–1326. [PubMed: 21481539]

Denver RJ. Structural and functional evolution of vertebrate neuroendocrine stress systems. Annals of the New York Academy of Sciences. 2009; 1163:1–16. [PubMed: 19456324]

Di S, Malcher-Lopes R, Marcheselli VL, Bazan NG, Tasker JG. Rapid glucocorticoid-mediated endocannabinoid release and opposing regulation of glutamate and gamma-aminobutyric acid inputs to hypothalamic magnocellular neurons. Endocrinology. 2005; 146(10):4292–4301. [PubMed: 15994343]

Encinas JM, Vaahtokari A, Enikolopov G. Fluoxetine targets early progenitor cells in the adult brain. Proceedings of the National Academy of Sciences of the United States of America. 2006; 103(21): 8233–8238. [PubMed: 16702546]

Figueiredo HF, Dolgas CM, Herman JP. Stress activation of cortex and hippocampus is modulated by sex and stage of estrus. Endocrinology. 2002; 143(7):2534–2540. [PubMed: 12072385]

Friend KE, Resnick EM, Ang LW, Shupnik MA. Specific modulation of estrogen receptor mRNA isoforms in rat pituitary throughout the estrous cycle and in response to steroid hormones. Molecular and Cellular Endocrinology. 1997; 131(2):147–155. [PubMed: 9296373]

Fuzesi T, Daviu N, Wamsteeker Cusulin JI, Bonin RP, Bains JS. Hypothalamic CRH neurons orchestrate complex behaviours after stress. Nature Communications. 2016; 7:11937.

Goncharova ND. Stress responsiveness of the hypothalamic-pituitary-adrenal axis: Age-related features of the vasopressinergic regulation. Frontiers in Endocrinology (Lausanne). 2013; 4:26.

Goto K, Zhao Y, Saito M, Tomura A, Morinaga H, Nomura M, … Nawata H. Activation function-1 domain of androgen receptor contributes to the interaction between two distinct subnuclear compartments. Journal of Steroid Biochemistry and Molecular Biology. 2003; 85(2–5):201–208. [PubMed: 12943705]

Griffin GD, Ferri-Kolwicz SL, Reyes BA, Van Bockstaele EJ, Flanagan-Cato LM. Ovarian hormone-induced reorganization of oxytocin-labeled dendrites and synapses lateral to the hypo-thalamic ventromedial nucleus in female rats. The Journal of Comparative Neurology. 2010; 518(22):4531–4545. [PubMed: 20886620]

Handa RJ, Burgess LH, Kerr JE, O'Keefe JA. Gonadal steroid hormone receptors and sex differences in the hypothalamo-pituitary-adrenal axis. Hormones and Behavior. 1994; 28(4):464–476. [PubMed: 7729815]

Handa RJ, Mani SK, Uht RM. Estrogen receptors and the regulation of neural stress responses. Neuroendocrinology. 2012; 96(2):111–118. [PubMed: 22538291]

Handa RJ, Weiser MJ. Gonadal steroid hormones and the hypothalamo-pituitary-adrenal axis. Frontiers in Neuroendocrinology. 2014; 35(2):197–220. [PubMed: 24246855]

Herman JP. Central mechanisms of stress integration: Hierarchical circuitry controlling hypothalamo-pituitary-adrenocortical responsiveness. Frontiers in Neuroendocrinology. 2003; 24:151–180. [PubMed: 14596810]

Hiroi R, Lacagnina AF, Hinds LR, Carbone DG, Uht RM, Handa RJ. The androgen metabolite, 5alpha-androstane-3beta,17beta-diol (3beta-diol), activates the oxytocin promoter through an estrogen receptor-beta pathway. Endocrinology. 2013; 154(5):1802–1812. [PubMed: 23515287]

Hrabovszky E, Kallo I, Steinhauser A, Merchenthaler I, Coen CW, Petersen SL, Liposits Z. Estrogen receptor-beta in oxytocin and vasopressin neurons of the rat and human hypothalamus: Immunocytochemical and in situ hybridization studies. The Journal of Comparative Neurology. 2004; 473(3):315–333. [PubMed: 15116394]

Jacome L, Gautreaux C, Inagaki T, Mohan G, Alves S, Lubbers L, Luine V. Estradiol and ERβ agonists enhance recognition memory, and DPN, an ERβ agonist, alters brain monoamines. Neurobiology of Learning and Memory. 2010; 94:488–498. [PubMed: 20828630]

Kadar A, Sanchez E, Wittmann G, Singru PS, Fuzesi T, Marsili A, … Fekete C. Distribution of hypophysiotropic thyrotropin-releasing hormone (TRH)-synthesizing neurons in the hypothalamic paraventricular nucleus of the mouse. The Journal of Comparative Neurology. 2010; 518(19): 3948–3961. [PubMed: 20737594]

Kasting NW, Martin JB. Changes in immunoreactive vasopressin concentrations in brain regions of the rat in response to endotoxin. Brain Research. 1983; 258(1):127–132. [PubMed: 24010175]

Kasting NW, Mazurek MF, Martin JB. Endotoxin increases vasopressin release independently of known physiological stimuli. The American Journal of Physiology. 1985; 248(4 Pt 1):E420–E424. [PubMed: 3885754]

Kiss A, Mravec B, Palkovits M, Kvetnansky R. Stress-induced changes in tyrosine hydroxylase gene expression in rat hypothalamic paraventricular, periventricular, and dorsomedial nuclei. Annals of the New York Academy of Sciences. 2008; 1148:74–85. [PubMed: 19120093]

Kiss JZ, Mezey E, Skirboll L. Corticotropin-releasing factor-immunoreactive neurons of the paraventricular nucleus become vasopressin positive after adrenalectomy. Proceedings of the

National Academy of Sciences of the United States of America. 1984; 81(6):1854–1858. [PubMed: 6608732]

Kriegsfeld LJ, Korets R, Silver R. Expression of the circadian clock gene Period 1 in neuroendocrine cells: An investigation using mice with a Per1::GFP transgene. The European Journal of Neuroscience. 2003; 17(2):212–220. [PubMed: 12542657]

Kruijver FP, Balesar R, Espila AM, Unmehopa UA, Swaab DF. Estrogen-receptor-beta distribution in the human hypothalamus: Similarities and differences with ER alpha distribution. The Journal of Comparative Neurology. 2003; 466(2):251–277. [PubMed: 14528452]

Kudwa AE, McGivern RF, Handa RJ. Estrogen receptor beta and oxytocin interact to modulate anxiety-like behavior and neuroendocrine stress reactivity in adult male and female rats. Physiology & Behavior. 2014; 129:287–296. [PubMed: 24631553]

Kuiper GG, Carlsson B, Grandien K, Enmark E, Haggblad J, Nilsson S, Gustafsson JA. Comparison of the ligand binding specificity and transcript tissue distribution of estrogen receptors alpha and beta. Endocrinology. 1997; 138(3):863–870. [PubMed: 9048584]

Kuiper GG, Enmark E, Pelto-Huikko M, Nilsson S, Gustafsson JA. Cloning of a novel receptor expressed in rat prostate and ovary. Proceedings of the National Academy of Sciences of the United States of America. 1996; 93(12):5925–5930. [PubMed: 8650195]

Laflamme N, Nappi RE, Drolet G, Labrie C, Rivest S. Expression and neuropeptidergic characterization of estrogen receptors (ERalpha and ERbeta) throughout the rat brain: anatomical evidence of distinct roles of each subtype. Journal of Neurobiology. 1998; 36:357–378. [PubMed: 9733072]

Li X, Schwartz PE, Rissman EF. Distribution of estrogen receptor-beta-like immunoreactivity in rat forebrain. Neuroendocrinology. 1997; 66(2):63–67. [PubMed: 9263202]

Lund TD, Hinds LR, Handa RJ. The androgen 5alpha-dihydrotestosterone and its metabolite 5alpha-androstan-3beta, 17beta-diol inhibit the hypothalamo-pituitary-adrenal response to stress by acting through estrogen receptor beta-expressing neurons in the hypothalamus. Journal of Neuroscience. 2006; 26(5):1448–1456. [PubMed: 16452668]

Lund TD, Rovis T, Chung WC, Handa RJ. Novel actions of estrogen receptor-beta on anxiety-related behaviors. Endocrinology. 2005; 146:797–807. [PubMed: 15514081]

Marques-Lopes J, Lynch MK, Van Kempen TA, Waters EM, Wang G, Iadecola C, … Milner TA. Female protection from slow-pressor effects of angiotensin II involves prevention of ROS production independent of NMDA receptor trafficking in hypothalamic neurons expressing angiotensin 1A receptors. Synapse. 2015; 69(3):148–165. [PubMed: 25559190]

Marques-Lopes J, Tesfaye E, Israilov S, Van Kempen TA, Wang G, Glass MJ, … Milner TA. Redistribution of NMDA receptors in estrogen-receptor-beta-containing paraventricular hypothalamic neurons following slow-pressor angiotensin II hypertension in female mice with accelerated ovarian failure. Neuroendocrinology. 2017; 104(3):239–256. [PubMed: 27078860]

Marques-Lopes J, Van Kempen T, Waters EM, Pickel VM, Iadecola C, Milner TA. Slow-pressor angiotensin II hypertension and concomitant dendritic NMDA receptor trafficking in estrogen receptor beta-containing neurons of the mouse hypothalamic paraventricular nucleus are sex and age dependent. The Journal of Comparative Neurology. 2014; 522(13):3075–3090. [PubMed: 24639345]

McCarthy MM, McDonald CH, Brooks PJ, Goldman D. An anxiolytic action of oxytocin is enhanced by estrogen in the mouse. Physiology & Behavior. 1996; 60(5):1209–1215. [PubMed: 8916173]

McClellan KM, Stratton MS, Tobet SA. Roles for gamma-aminobutyric acid in the development of the paraventricular nucleus of the hypothalamus. The Journal of Comparative Neurology. 2010; 518(14):2710–2728. [PubMed: 20506472]

Miller WJ, Suzuki S, Miller LK, Handa R, Uht RM. Estrogen receptor (ER)beta isoforms rather than ERalpha regulate corticotropin-releasing hormone promoter activity through an alternate pathway. The Journal of Neuroscience. 2004; 24(47):10628–10635. [PubMed: 15564578]

Milner TA, Thompson LI, Wang G, Kievits JA, Martin E, Zhou P, … Waters EM. Distribution of estrogen receptor β containing cells in the brains of bacterial artificial chromosome transgenic mice. Brain Research. 2010; 1351:74–96. [PubMed: 20599828]

Muller MB, Preil J, Renner U, Zimmermann S, Kresse AE, Stalla GK, … Wurst W. Expression of CRHR1 and CRHR2 in mouse pituitary and adrenal gland: Implications for HPA system regulation. Endocrinology. 2001; 142(9):4150–4153. [PubMed: 11517194]

Neumann ID, Krömer SA, Toschi N, Ebner K. Brain oxytocin inhibits the (re)activity of the hypothalamo-pituitary-adrenal axis in male rats: Involvement of hypothalamic and limbic brain regions. Regulatory Peptides. 2000a; 96:31–38. [PubMed: 11102649]

Neumann ID, Wigger A, Torner L, Holsboer F, Landgraf R. Brain oxytocin inhibits basal and stress-induced activity of the hypothalamo-pituitary-adrenal axis in male and female rats: partial action within the paraventricular nucleus. Journal of Neuroendocrinology. 2000b; 12(3):235–243. [PubMed: 10718919]

Nomura M. Estrogen receptor-β regulates transcript levels for oxytocin and arginine vasopressin in the hypothalamic para-ventricular nucleus of male mice. Molecular Brain Research. 2002; 109:84–94. [PubMed: 12531518]

Ochedalski T, Subburaju S, Wynn PC, Aguilera G. Interaction between oestrogen and oxytocin on hypothalamic-pituitary-adrenal axis activity. Journal of Neuroendocrinology. 2007; 19:189–197. [PubMed: 17280592]

Oyola MG, Portillo W, Reyna A, Foradori CD, Kudwa A, Hinds L, … Mani SK. Anxiolytic effects and neuroanatomical targets of estrogen receptor-beta (ERbeta) activation by a selective ERbeta agonist in female mice. Endocrinology. 2011; 153(2):837–846. [PubMed: 22186418]

Pak TR, Chung WC, Hinds LR, Handa RJ. Estrogen receptor-beta mediates dihydrotestosterone-induced stimulation of the arginine vasopressin promoter in neuronal cells. Endocrinology. 2007; 148(7):3371–3382. [PubMed: 17412808]

Papka RE, Storey-Workley M. Estrogen receptor-alpha and -beta coexist in a subpopulation of sensory neurons of female rat dorsal root ganglia. Neuroscience Letters. 2002; 319(2):71–74. [PubMed: 11825673]

Patisaul HB, Scordalakes EM, Young LJ, Rissman EF. Oxytocin, but not oxytocin receptor, is regulated by oestrogen receptor beta in the female mouse hypothalamus. Journal of Neuroendocrinology. 2003; 15:787–793. [PubMed: 12834440]

Richard S, Zingg HH. The human oxytocin gene promoter is regulated by estrogens. The Journal of Biological Chemistry. 1990; 265(11):6098–6103. [PubMed: 2108152]

Rissman EF, Heck AL, Leonard JE, Shupnik MA, Gustafsson JA. Disruption of estrogen receptor beta gene impairs spatial learning in female mice. Proceedings of the National Academy of Sciences of the United States of America. 2002; 99(6):3996–4001. [PubMed: 11891272]

Saper CB, Sawchenko PE. Magic peptides, magic antibodies: Guidelines for appropriate controls for immunohistochemistry. The Journal of Comparative Neurology. 2003; 465(2):161–163. [PubMed: 12949777]

Sawchenko PE, Swanson LW, Vale WW. Corticotropin-releasing factor: Co-expression within distinct subsets of oxytocin-, vasopressin-, and neurotensin-immunoreactive neurons in the hypothalamus of the male rat. The Journal of Neuroscience. 1984; 4(4):1118–1129. [PubMed: 6609226]

Shapiro RA, Xu C, Dorsa DM. Differential transcriptional regulation of rat vasopressin gene expression by estrogen receptor alpha and beta. Endocrinology. 2000; 141(11):4056–4064. [PubMed: 11089536]

Shughrue PJ, Komm B, Merchenthaler I. The distribution of estrogen receptor-beta mRNA in the rat hypothalamus. Steroids. 1996; 61:678–681. [PubMed: 8987135]

Shughrue PJ, Merchenthaler I. Distribution of estrogen receptor beta immunoreactivity in the rat central nervous system. The Journal of Comparative Neurology. 2001; 436(1):64–81. [PubMed: 11413547]

Sladek CD, Somponpun SJ. Estrogen receptors: Their roles in regulation of vasopressin release for maintenance of fluid and electrolyte homeostasis. Frontiers in Neuroendocrinology. 2008; 29(1): 114–127. [PubMed: 18022678]

Smith JA, Wang L, Hiller H, Taylor CT, de Kloet AD, Krause EG. Acute hypernatremia promotes anxiolysis and attenuates stress-induced activation of the hypothalamic-pituitary-adrenal axis in male mice. Physiology & Behavior. 2014; 136:91–96. [PubMed: 24704193]

Snyder MA, Smejkalova T, Forlano PM, Woolley CS. Multiple ERbeta antisera label in ERbeta knockout and null mouse tissues. Journal of Neuroscience Methods. 2010; 188(2):226–234. [PubMed: 20170675]

Solum DT, Handa RJ. Estrogen regulates the development of brain-derived neurotrophic factor mRNA and protein in the rat hippocampus. The Journal of Neuroscience. 2002; 22(7):2650–2659. [PubMed: 11923430]

Somponpun SJ, Sladek CD. Osmotic regulation of estrogen receptor-beta in rat vasopressin and oxytocin neurons. The Journal of Neuroscience. 2003; 23(10):4261–4269. [PubMed: 12764114]

Somponpun SJ, Sladek CD. Depletion of oestrogen receptor-beta expression in magnocellular arginine vasopressin neurones by hypovolaemia and dehydration. Journal of Neuroendocrinology. 2004; 16(6):544–549. [PubMed: 15189329]

Stern JE, Zhang W. Preautonomic neurons in the paraventricular nucleus of the hypothalamus contain estrogen receptor beta. Brain Research. 2003; 975(1–2):99–109. [PubMed: 12763597]

Sutton AK, Pei H, Burnett KH, Myers MG Jr, Rhodes CJ, Olson DP. Control of food intake and energy expenditure by Nos1 neurons of the paraventricular hypothalamus. The Journal of Neuroscience. 2014; 34(46):15306–15318. [PubMed: 25392498]

Suzuki S, Handa RJ. Regulation of estrogen receptor-beta expression in the female rat hypothalamus: Differential effects of dexamethasone and estradiol. Endocrinology. 2004; 145(8):3658–3670. [PubMed: 15087431]

Suzuki S, Handa RJ. Estrogen receptor-beta, but not estrogen receptor-alpha, is expressed in prolactin neurons of the female rat paraventricular and supraoptic nuclei: Comparison with other neuropeptides. Journal of Comparative Neurology. 2005; 484:28–42. [PubMed: 15717309]

Swanson LW, Sawchenko PE. Paraventricular nucleus: A site for the integration of neuroendocrine and autonomic mechanisms. Neuroendocrinology. 1980; 31(6):410–417. [PubMed: 6109264]

Tanoue A, Ito S, Honda K, Oshikawa S, Kitagawa Y, Koshimizu TA, … Tsujimoto G. The vasopressin V1b receptor critically regulates hypothalamic-pituitary-adrenal axis activity under both stress and resting conditions. Journal of Clinical Investigation. 2004; 113(2):302–309. [PubMed: 14722621]

Thammacharoen S, Geary N, Lutz TA, Ogawa S, Asarian L. Divergent effects of estradiol and the estrogen receptor-alpha agonist PPT on eating and activation of PVN CRH neurons in ovariectomized rats and mice. Brain Research. 2009; 1268:88–96. [PubMed: 19281799]

Vacher CM, Fretier P, Creminon C, Calas A, Hardin-Pouzet H. Activation by serotonin and noradrenaline of vasopressin and oxytocin expression in the mouse paraventricular and supraoptic nuclei. The Journal of Neuroscience. 2002; 22(5):1513–1522. [PubMed: 11880481]

Volkmann K, Chen YY, Harris MP, Wullimann MF, Koster RW. The zebrafish cerebellar upper rhombic lip generates teg-mental hindbrain nuclei by long-distance migration in an evolutionary conserved manner. The Journal of Comparative Neurology. 2010; 518(14):2794–2817. [PubMed: 20506476]

Wamsteeker Cusulin JI, Fuzesi T, Watts AG, Bains JS. Characterization of corticotropin-releasing hormone neurons in the paraventricular nucleus of the hypothalamus of Crh-IRES-Cre mutant mice. PloS One. 2013; 8(5):e64943. [PubMed: 23724107]

Wasserman DI, Wang HG, Rashid AJ, Josselyn SA, Yeomans JS. Cholinergic control of morphine-induced locomotion in rostromedial tegmental nucleus versus ventral tegmental area sites. The European Journal of Neuroscience. 2013; 38(5):2774–2785. [PubMed: 23773170]

Weiser MJ, Handa RJ. Estrogen impairs glucocorticoid dependent negative feedback on the hypothalamic-pituitary-adrenal axis via estrogen receptor alpha within the hypothalamus. Neuroscience. 2009; 159(2):883–895. [PubMed: 19166915]

Weiser MJ, Wu TJ, Handa RJ. Estrogen receptor-beta agonist diarylpropionitrile: Biological activities of R- and S-enantiomers on behavior and hormonal response to stress. Endocrinology. 2009; 150(4):1817–1825. [PubMed: 19074580]

Whitnall MH. Stress selectively activates the vasopressin-containing subset of corticotropin-releasing hormone neurons. Neuroendocrinology. 1989; 50(6):702–707. [PubMed: 2515467]

Windle RJ, Kershaw YM, Shanks N, Wood SA, Lightman SL, Ingram CD. Oxytocin attenuates stress-induced c-fos mRNA expression in specific forebrain regions associated with modulation of

hypothalamo-pituitary-adrenal activity. The Journal of Neuroscience. 2004; 24:2974–2982. [PubMed: 15044536]

Zuloaga DG, Zuloaga KL, Hinds LR, Carbone DL, Handa RJ. Estrogen receptor beta expression in the mouse forebrain: Age and sex differences. The Journal of Comparative Neurology. 2014; 522(2): 358–371. [PubMed: 23818057]

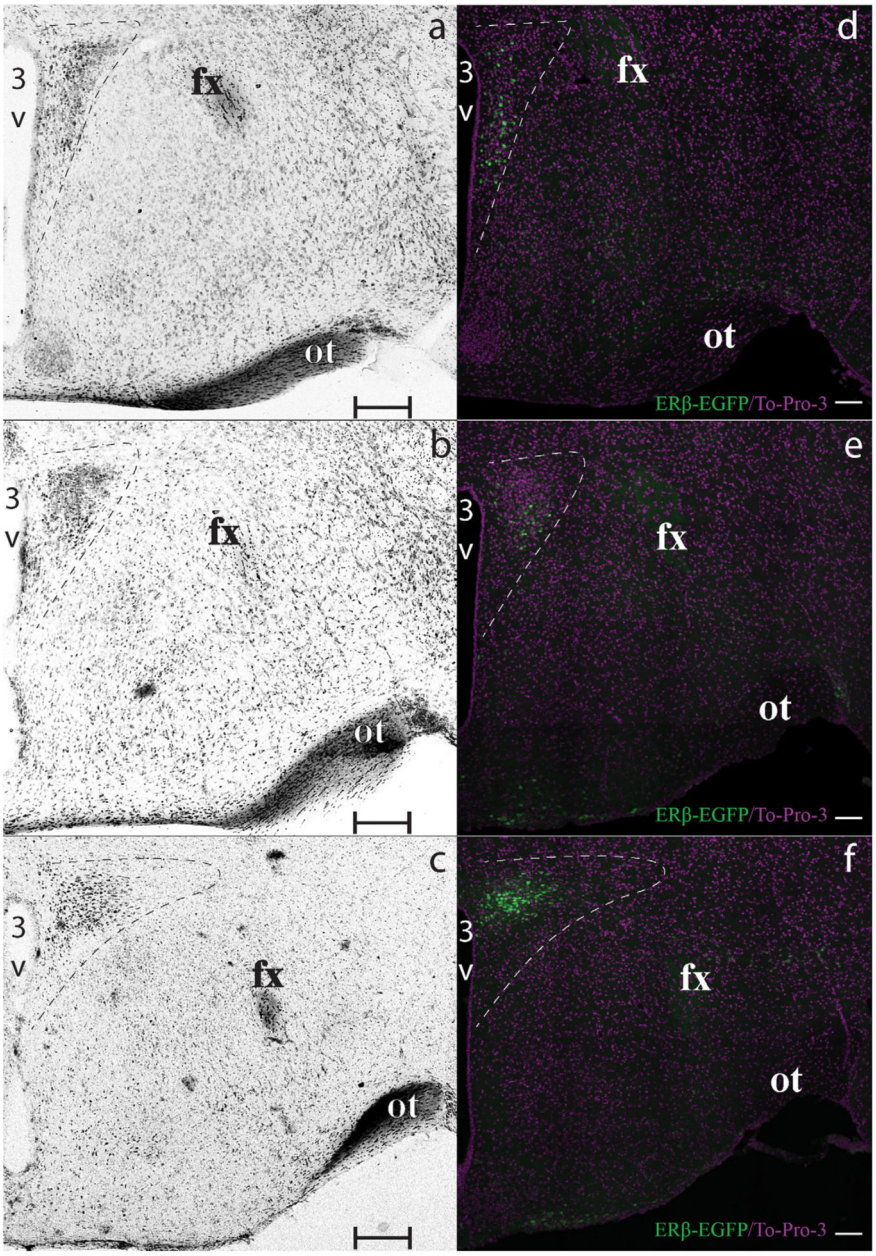

FIGURE 1.

ERβ-EGFP PVN rostrocaudal partition. Photomicrographs showing bright-field Nissl (a–c) and confocal (d–f) images demonstrate the rostral (a, d), middle (b, e) and caudal (c, f) regions of the PVN, which are delineated using a white dashed line. Brain sections are presented rostrocaudally using the Nissl-stained edges (a–c) as the defining borders of the PVN at each level examined. Representative ERβ-EGFP (green) signal images matching the respective rostrocaudal level are shown in panels (d–f). Nuclear ir (To-Pro-3) for contrast is represented in magenta. Scale bars: (a–c) = 200 μm, (d–f) = 100 μm. 3V, Third ventricle. fx, fornix. ot, optic tract [Color figure can be viewed at wileyonlinelibrary.com]

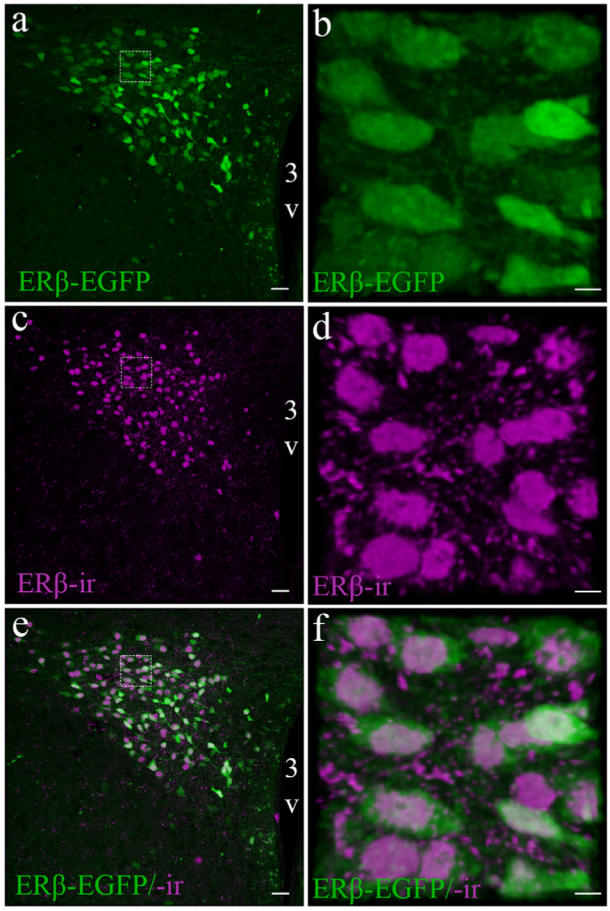

FIGURE 2.

Validation of the ERβ-EGFP mouse model for studying PVN ERβ expression. Representative confocal photomicrographs comparing the distribution of ERβ-EGFP in a female mouse (similar pattern is observed in males) (a) with ERβ-ir (c), using the Z8P antibody in the middle-caudal PVN. Enlarged images (b, d, f) shows a higher power view demonstrating the distribution of ERβ-EGFP (green) and ERβ-ir cells (magenta). And their colocalization (e, f). For all high power insets (dotted line box) the scale bar = 10 μm. Scale bars for all other images = 50 μm. 3V, Third ventricle [Color figure can be viewed at wileyonlinelibrary.com]

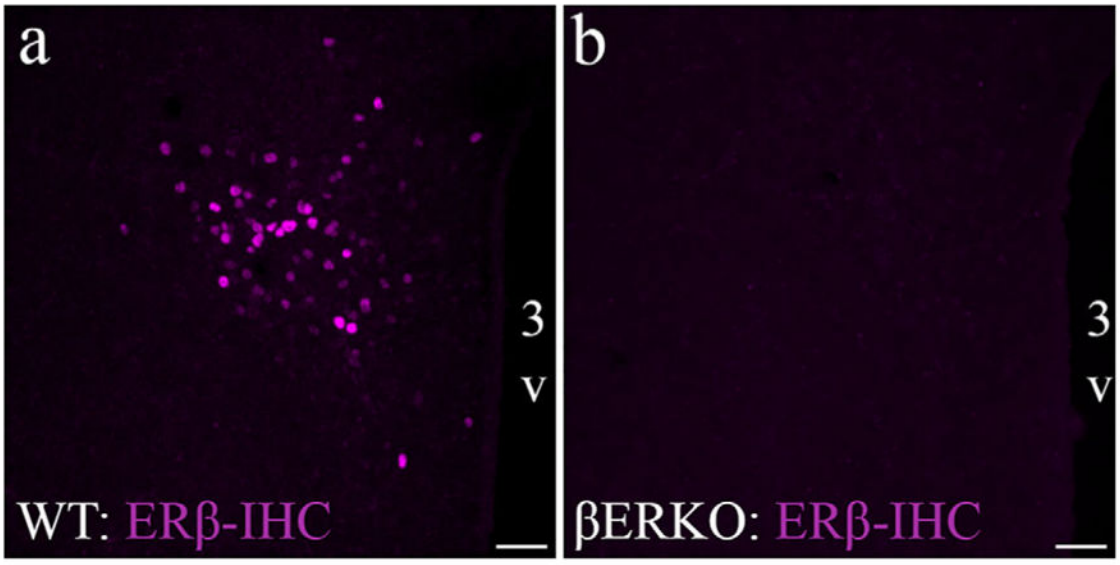

FIGURE 3.

ERβ Z8P antibody validation using the global ERβ knockout mouse model. Photomicrographs showing ERβ-ir in PVN of wildtype (WT; a) and global ERβ knockout (βERKO; b) following IHC using the Z8P antibody (magenta). Scale bars = 50 μm. 3V, Third ventricle [Color figure can be viewed at wileyonlinelibrary.com]

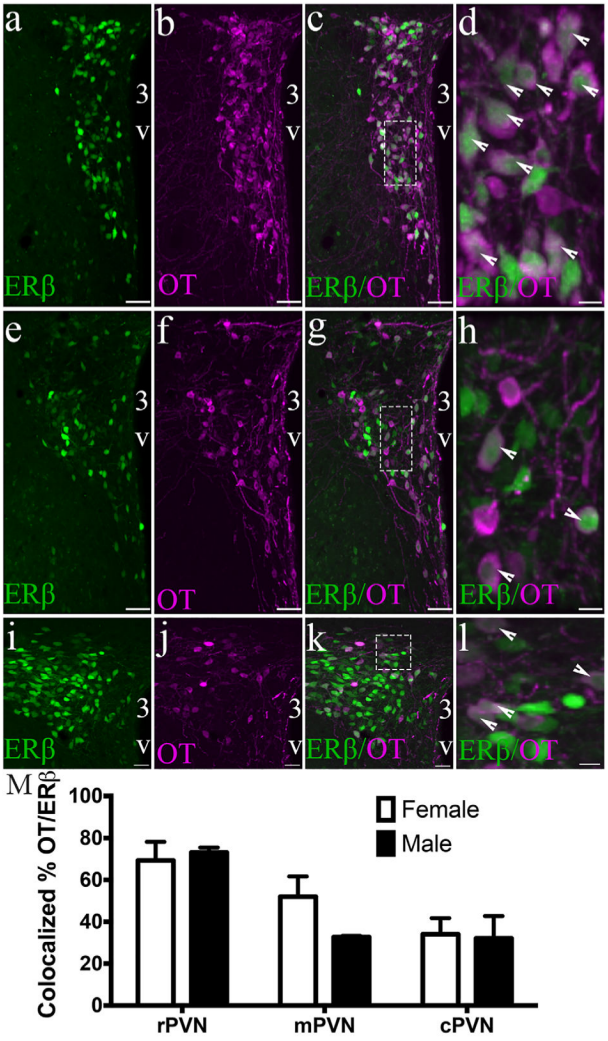

FIGURE 4.

OT colocalizes with PVN ERβ-EGFP cells in an PVN region-specific manner. Representative confocal photomicrographs of a female ERβ-EGFP mouse showing rostral (a–d), middle (e–h), and caudal (i–l) PVN oxytocin (OT) immunoreactivity and ERβ-EGFP (n = 3/sex). Bar graph (m) show the mean percentage colocalization of OT in ERβ-EGFP neurons in the rPVN, mPVP, and rPVN of male and female mice (m). % colocalization = number of OT-ir neurons/total number of ERβ neurons in selected region × 100. Data are expressed as mean percentage ± *SEM*. For all higher power (dotted line box) images (d, h, l) the scale bar = 10 μm. Scale bars for all other images = 50 μm. 3V, Third ventricle. Arrowheads show examples of double labeled cells [Color figure can be viewed at wileyonlinelibrary.com]

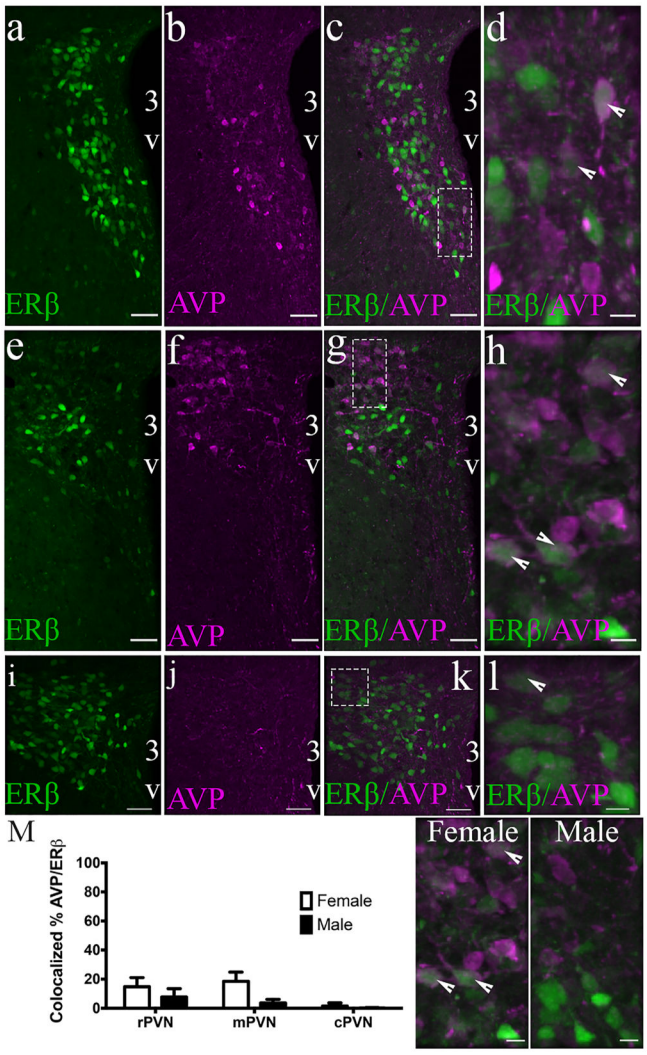

FIGURE 5.

PVN ERβ-EGFP cells express AVP. Photomicrographs of a female ERβ-EGFP mouse showing rostral (a–d), middle (e–h), and caudal (i–l) AVP immunoreactivity in the PVN of ERβ-EGFP brain slices (n = 3–4/sex). Bar graphs (m) show the mean percentage colocalization of AVP in ERβ-EGFP neurons in the rPVN, mPVP, and rPVN of male and female mice. Representative male and female photomicrographs showing distribution of colocalized and non-colocalized cells in the mPVN. % colocalization = number of AVP-ir neurons/total number of EGFP neurons in each selected region. Data are expressed as mean percentage ± *SEM*. For all high power (dotted line box) images (d, h, l) the scale bar = 10 μm. Scale bars for all other images = 50 μm. 3V, Third ventricle. Arrowheads show examples of colocalized cells [Color figure can be viewed at wileyonlinelibrary.com]

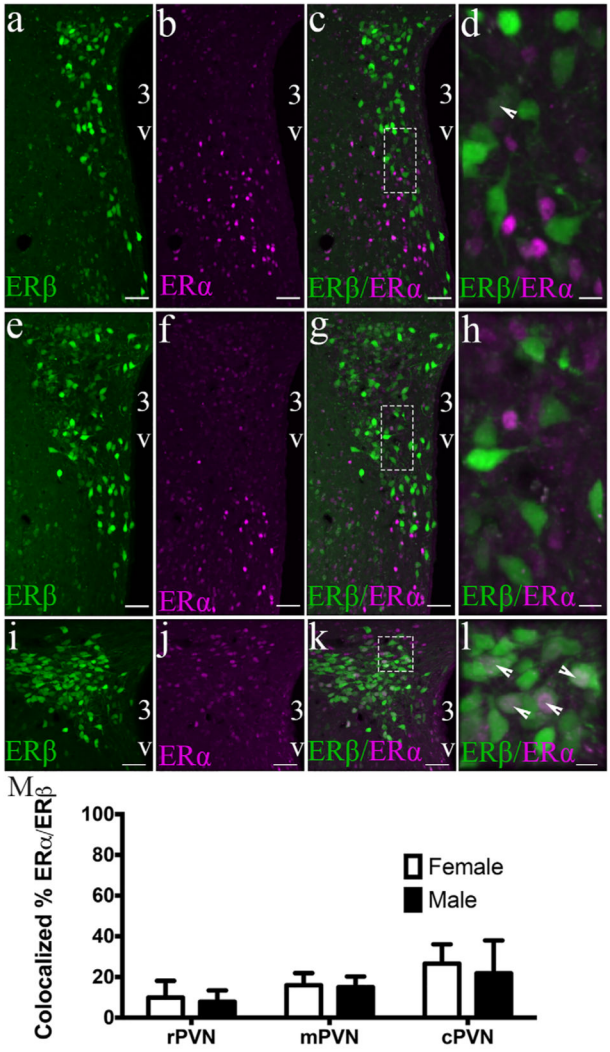

FIGURE 6.

ERα/ERβ-EGFP colocalized cells are present in low levels in the male and female mouse PVN. Photomicrographs of a female ERβ-EGFP mouse showing ERα immunoreactivity (magenta) in the rostral (a–d), middle (e–h), and caudal (i–l) parts of the PVN of ERβ-EGFP animals (n = 3–4/sex). Bar graphs (panel m) represent the mean percentage colocalization of ERα in ERβ-EGFP neurons of male and female mice. % colocalization = number of colocalized ERα/total number of ERβ neurons in selected region. Data are expressed as mean percentage ± *SEM*. For all high-power images (dotted line box) (d, h, l) the scale bar = 10 μm. Scale bars for all other images = 50 μm. 3V, Third ventricle. Arrowheads show examples of dual labeled cells [Color figure can be viewed at wileyonli-nelibrary.com]

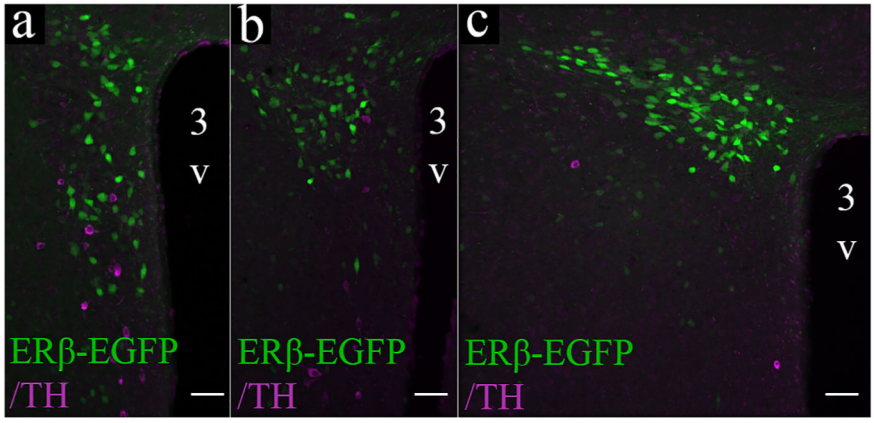

FIGURE 7.

ERβ-EGFP neurons do not colocalize with TH-ir neurons in the mouse PVN. Photomicrographs showing overlayed confocal images of the PVN through the rostral (a), middle (b), and caudal (c) regions of an ERβ-EGFP female mouse. Scale bars = 50 μm. 3V, Third ventricle [Color figure can be viewed at wileyonlinelibrary.com]

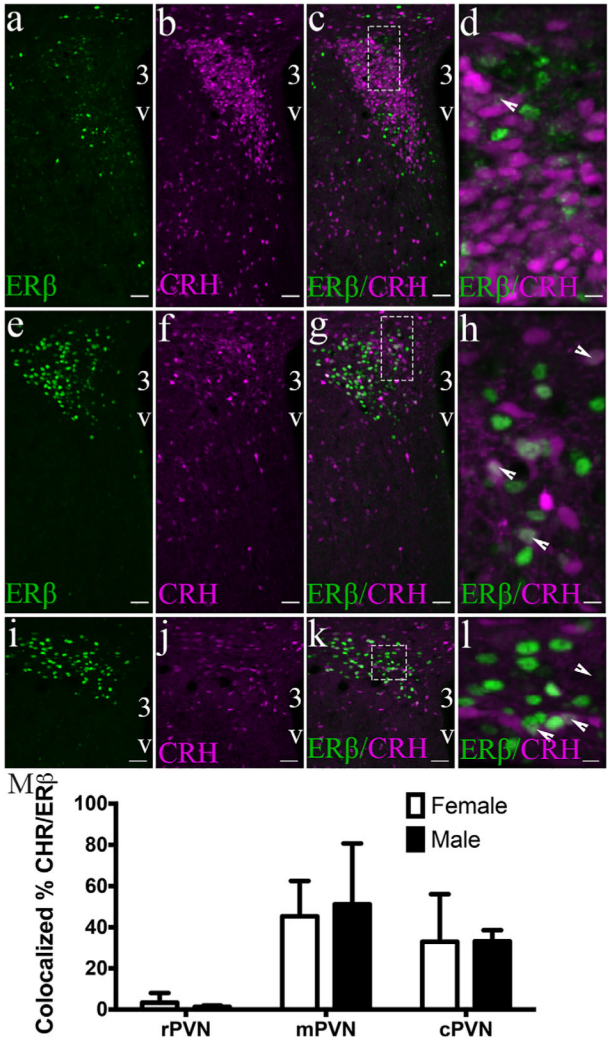

FIGURE 8.

CRH-tdTomato cells co-express ERβ-ir in the male and female mouse PVN. Photomicrographs of a male CRH-cre; TdTomato mouse showing confocal images of the PVN through the rostral (ad), middle (e–h), and caudal (i–l) regions of CRH-cre;TdTomato animals. ERβ immunoreactivity was detected using the Z8P antibody (n = 3/sex). Bar graphs (m) representing the mean percentage colocalization of CRH-TdTomato expressing neurons and ERβ-ir neurons in the rPVN, mPVP, and rPVN of male and female mice. % colocalization = number of TdTom positive neurons/total number of ERβ-ir neurons in selected region. Data are expressed as the mean percentage ± *SEM*. All higher power images (dotted line box) (d, h, l) have a scale bar = 10 μm. Scale bars for all other images = 50 μm. 3V, Third ventricle. Arrowheads show examples of a dual labeled cell [Color figure can be viewed at wileyonlinelibrary.com]

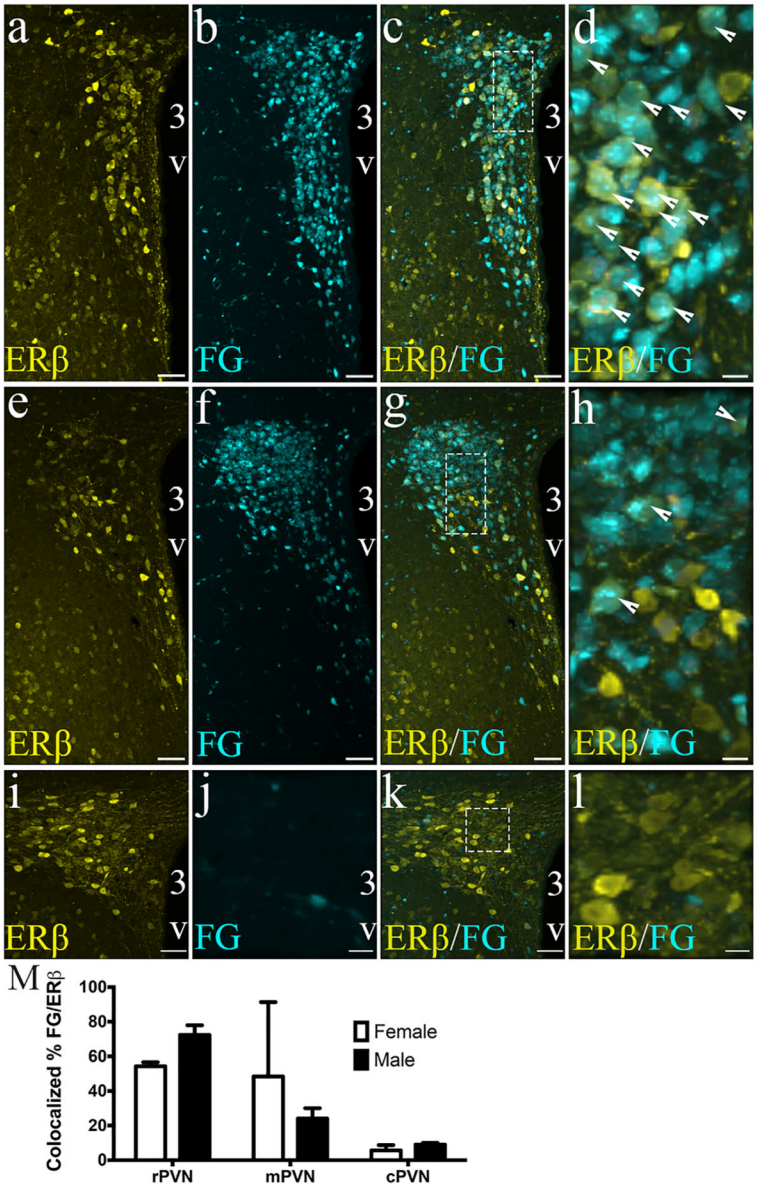

FIGURE 9.

ERβ-EGFP neurons are neuroendocrine neurons in the rostral but not caudal portions of the PVN. Confocal photomicrographs of a female ERβ-EGFP mouse showing the distribution of fluorogold (neuroendocrine) neurons in the rostral (a–d), middle (e–h), and caudal (i–l) portions of the PVN of ERβ-EGFP brain slices (n = 3–4/sex). EGFP was detected using an anti-GFP antibody. Fluorogold neurons were filled via subcutaneous injection of FG 5 days prior to euthanasia and harvesting the brain. Bar graph (m) represent the mean percentage colocalization of FG in ERβ-EGFP-ir neurons in the rPVN, mPVP, and rPVN of male and female mice. % colocalization = number of FG positive cells/total number of ERβ-EGFP-ir × 100. Data are expressed as mean percentage ± *SEM*. All high-power images (dotted line box) (d, h, l) have a scale bar = 10 μm. Scale bars for all other images = 50 μm. 3V, Third

ventricle. Arrowheads show examples of dual labeled cells [Color figure can be viewed at wileyonlinelibrary.com]

TABLE 1

Validation of antibodies used

Primary antibodies				
Target	**Antigen**	**Source**	**Working dilution**	**Reference**
Arginine vasopressin	Full length AVP peptide	Dr. James Koenig (Univ. MD) Rabbit polyclonal	1:2,500	Kasting and Martin (1983), Kasting et al. (1985)
Estrogen receptor α	Rat ERα C-term	Upstate #06–935 Rabbit polyclonal	1:5,000	Suzuki and Handa (2005), Cao et al. (2014), RRID:AB_310305
Estrogen receptor β	ERβ mC-term (468–485)	Zymed Z8P (no longer available) rabbit polyclonal	1:1,000	Shughrue and Merchenthaler (2001), Suzuki and Handa (2005), McClellan et al. (2010)
GFP	GFP-1020	Aves: Chicken polyclonal	1:1,000	Cao et al. (2014), RRID:AB_10000240
Oxytocin	Full length OT peptide	Peninsula: T4084 rabbit polyclonal	1:5,000	Sutton et al. (2014)
Tyrosine hydroxylase	Synthetic rat TH aa: 32–46	Abcam: ab6211: rabbit polyclonal	1:1,000	Wasserman, Wang, Rashid, Josselyn, and Yeomans (2013). RRID:AB_2240393
Secondary antibodies				
Antibody		**Source**	**Catalog No.**	**Working dilution**
Goat anti-Chicken IgY (H&L)DyLight® 594		ThermoFisher	SA5–10072	1:500 RRID:AB_2556652
Goat anti-Rabbit IgG (H&L) AlexaFluor® 594		Life Technologies	A-11037	1:500 RRID:AB_2534095
Goat biotinylated anti-rabbit IgG (H+L)		Vector Laboratories	BA-1000	1:500 RRID: AB_2313606
Streptavidin DyLight® 594		Vector Laboratories	SA5594	1:500 RRID:AB_2336418
TSA Fluorescein		Perkin Elmer	NEL744001KT	1:50
TSA Cy3		Perkin Elmer	NEL744001KT	1:50
ABC Kit Biotinylated/SA-HRP		Vector	PK-6104	RRID:AB_2336823